Journal of Geophysical Research-Oceans

Supporting Information for

Attribution and predictability of climate-driven variability in global ocean color

Hyung-Gyu Lim[1,2*], John P. Dunne[3], Charles A. Stock[3], Minho Kwon[4]

[1]Princeton University/Atmospheric and Oceanic Sciences Program, Princeton, NJ, USA

[2]Scripps Institution of Oceanography, University of California San Diego, CA, USA

[3]NOAA/OAR/Geophysical Fluid Dynamics Laboratory, Princeton, NJ, USA

[4]Korea Institute Ocean Science and Technology, Busan, South Korea

[*]Corresponding author: Hyung-Gyu Lim (hyl021@ucsd.edu)

Contents of this file

Introduction

This supporting information further provides comparisons of sets of three different merging algorithm based satellite ocean color datasets (GlobColour-GSM, GlobColour-AVM, and ESA-OC-CCI-v5.0) to estimate the surface chlorophyll concentration: Linear trends (Fig. S1), Seasonal cycle contribution on total chlorophyll variance (TCV) (Fig. S2), Contribution of both seasonal cycle and climate variability (considering instantaneous and delayed effects) on TCV (Fig. S3), Contribution of both seasonal cycle and climate variability (considering instantaneous effect only) on TCV (Fig. S4), predictability skills (Fig. S5), Areas of oligotrophic water (Fig. S6), Residual of explained TCV by seasonal cycle and climate variability (Fig. S7), and indication of lead-time for predicted chlorophyll anomaly (rCHLa_predic) shown in Fig. 5 of the main manuscript (Table S1).

Supporting figures

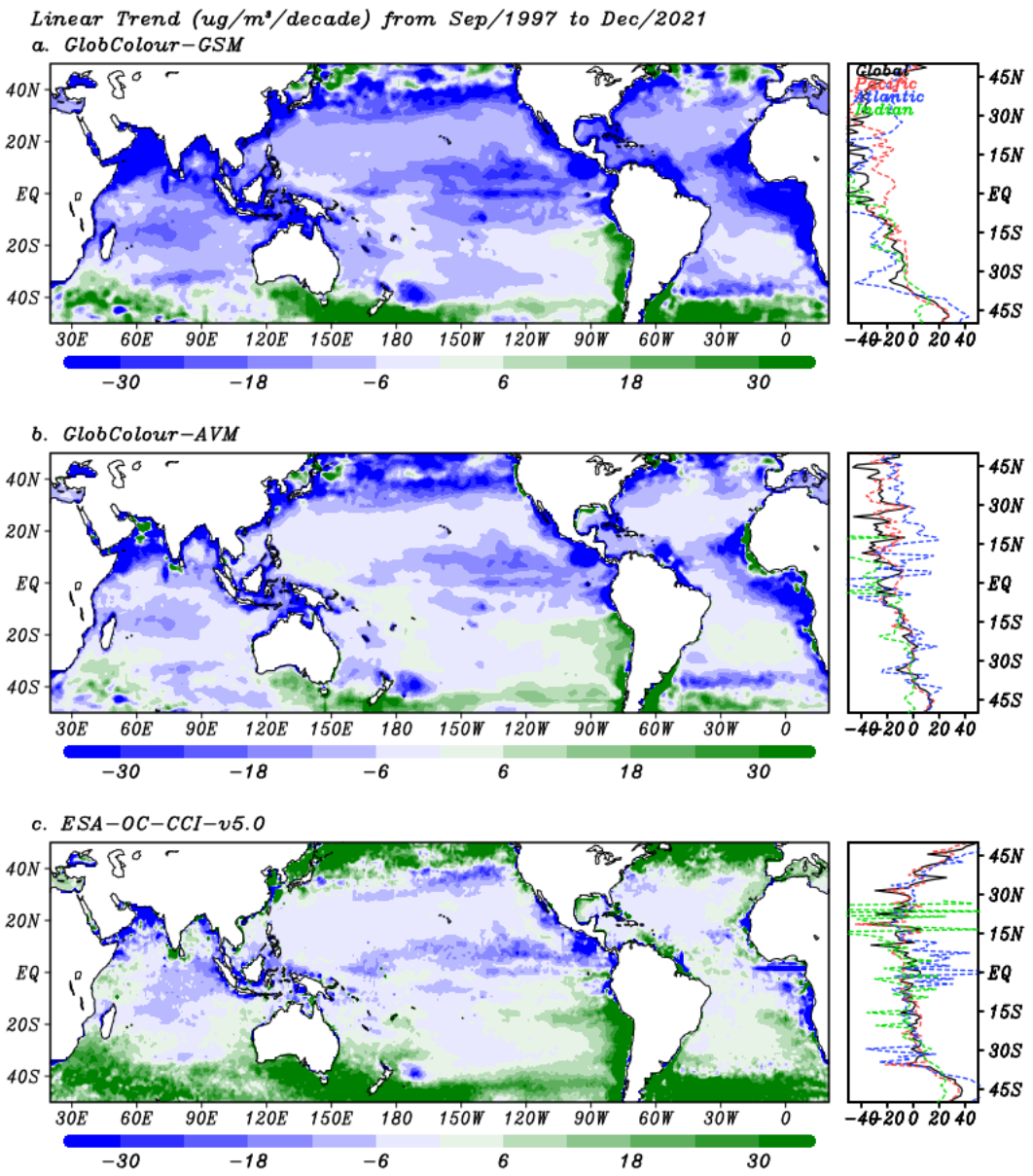

Figure S1. Linear trends of chlorophyll concentration in a. GlobColour-GSM, b. GlobColour-AVM, and c. ESA-OC-CCI-v5.0.

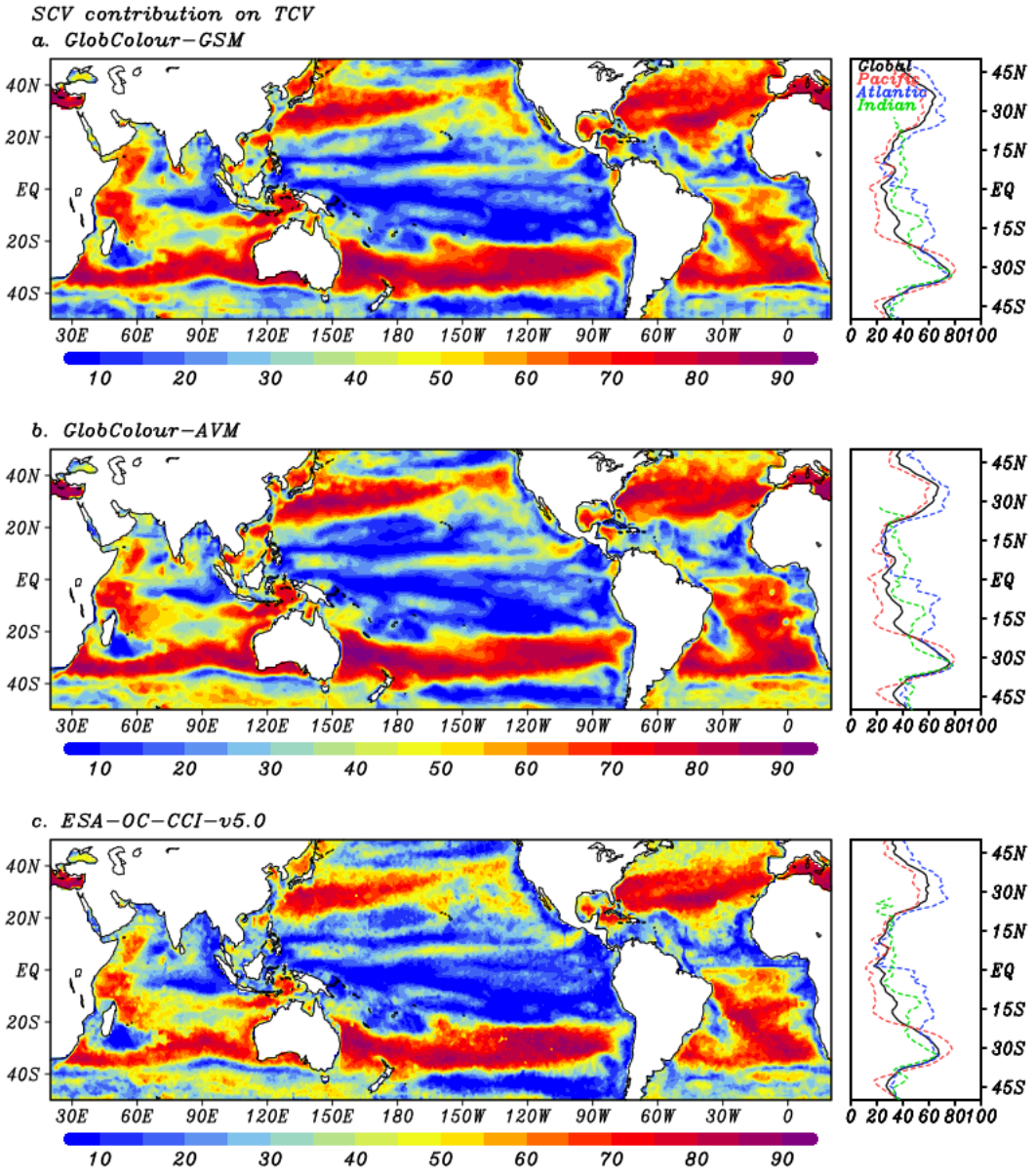

Figure S2. Contribution of SCV on TCV in a. GlobColour-GSM (same as Fig. 1c), b. GlobColour-AVM, and c. ESA-OC-CCI-v5.0.

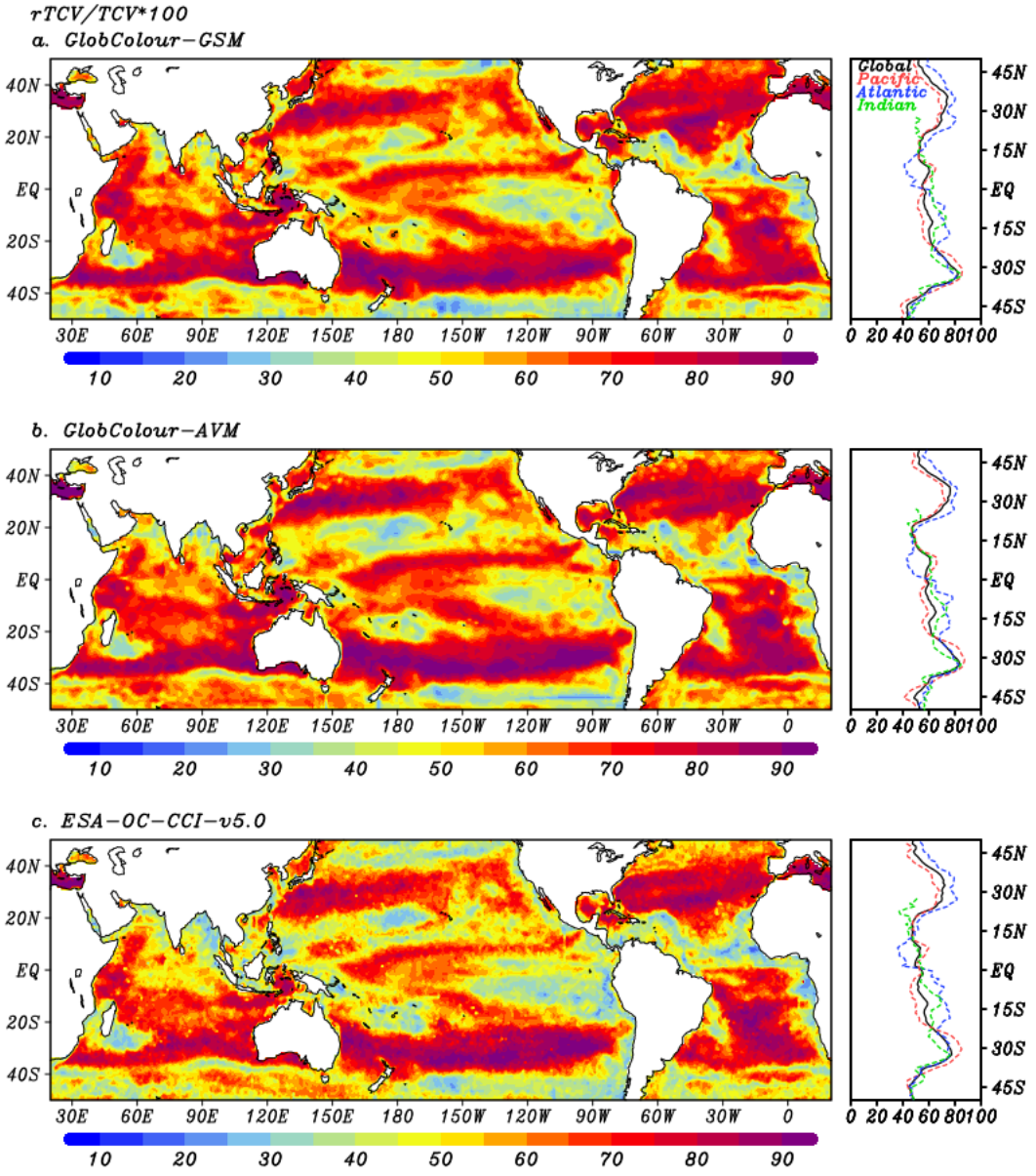

Figure S3. Explained TCV by rTCV in a. GlobColour-GSM (same as Fig. 2c), b. GlobColour-AVM, and c. ESA-OC-CCI-v5.0.

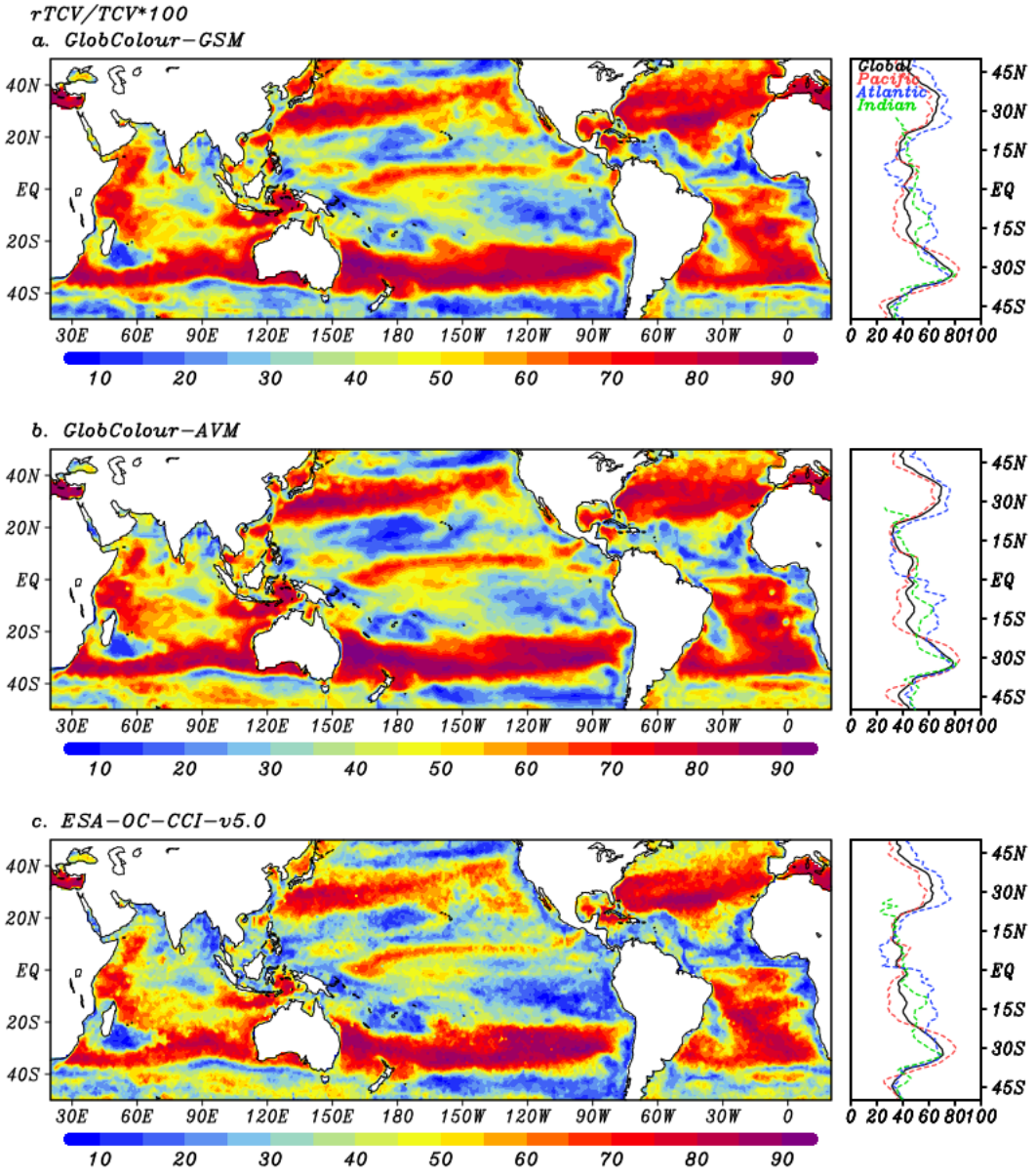

Figure S4. Explained TCV by rTCV, but only based on instantaneous effect of climate-driven variability in a. GlobColour-GSM, b. GlobColour-AVM, and c. ESA-OC-CCI-v5.0.

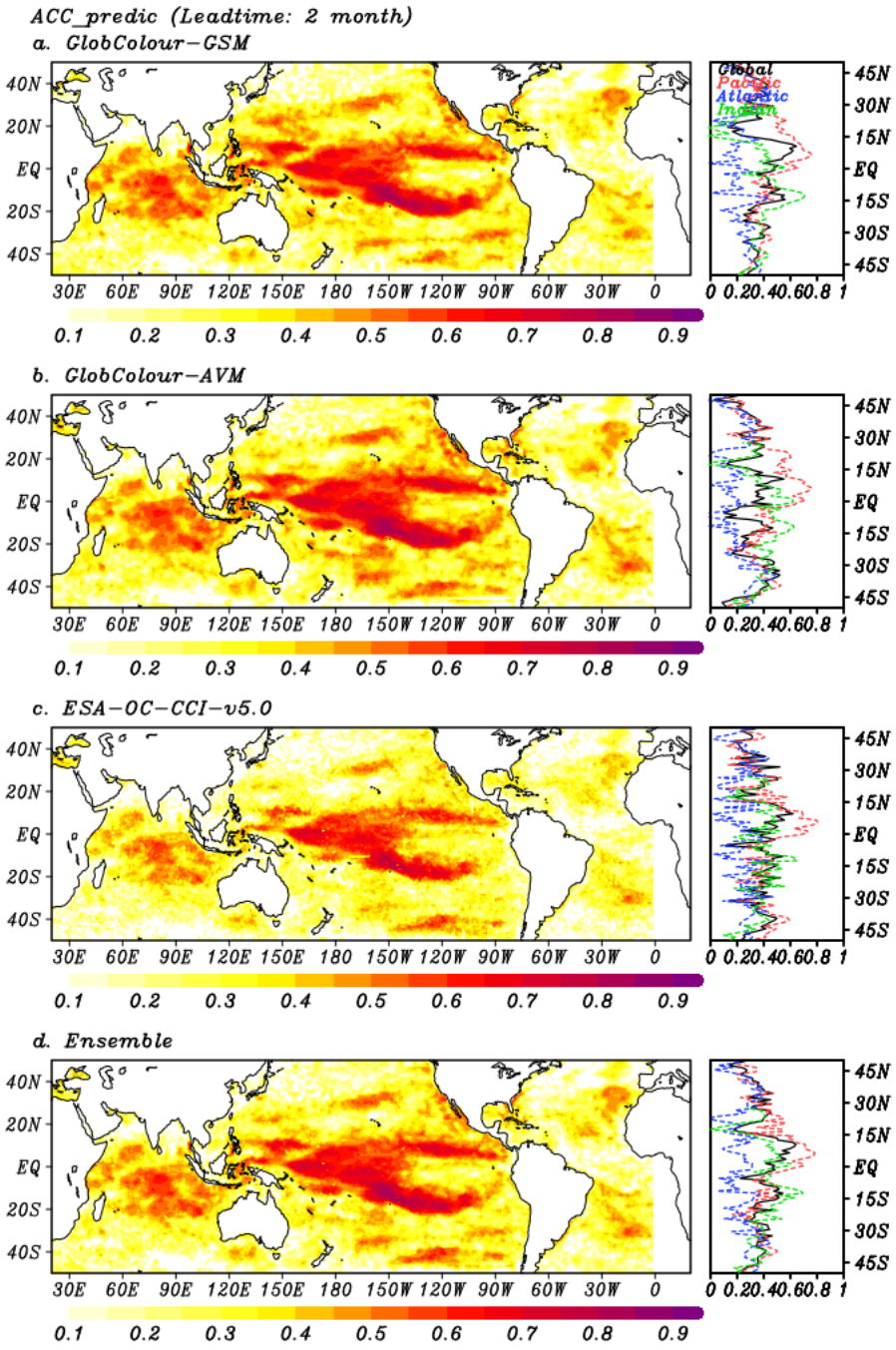

Figure S5. ACC_predic (Leadtime: 2 month) in a. GlobColour-GSM, b. GlobColour-AVM, c. ESA-OC-CCI-v5.0, and d. ensemble mean result based on averaged all satellite datasets (Glob-Colour-GSM, GlobColour-AVM, ESA-OC-CCI-v5.0).

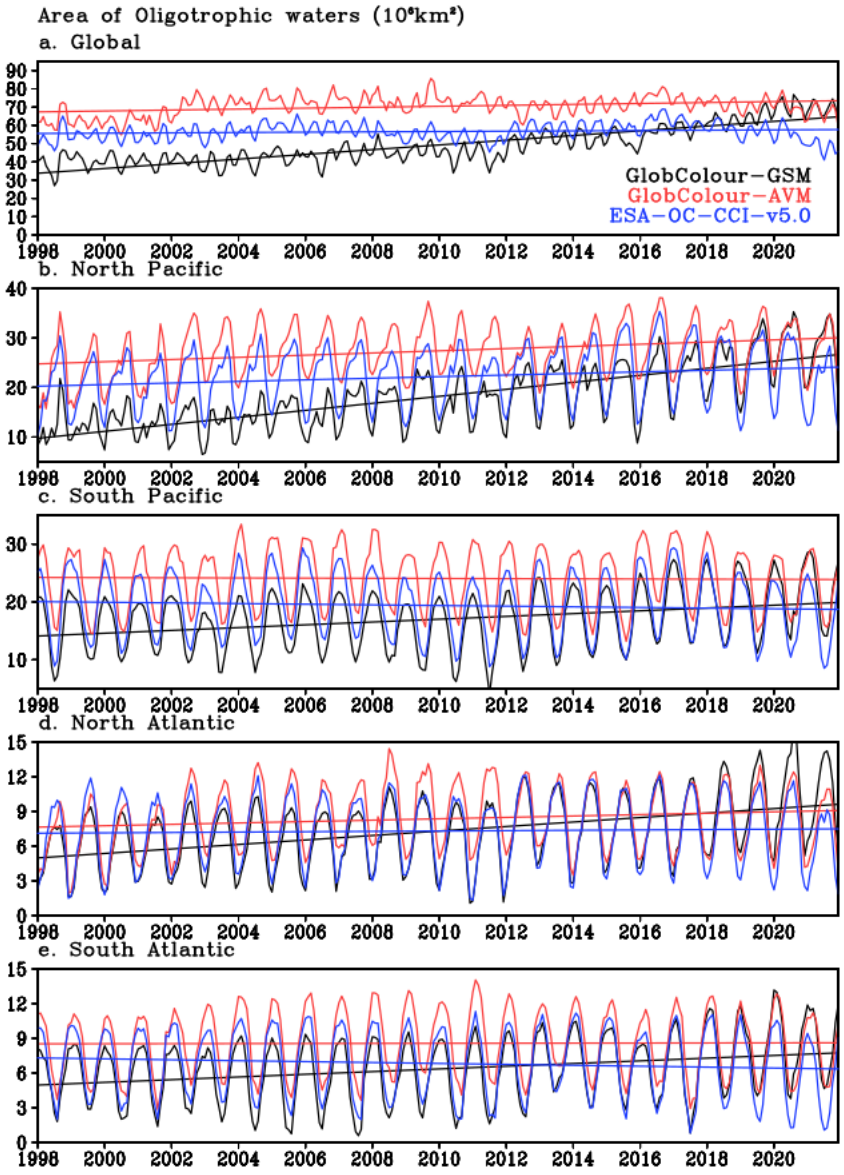

Figure S6. Timeseries of the monthly mean areas of oligotrophic waters (10^6 km^2) with surface chlorophyll less than 0.07 mg/m^3 between 5°-45° N/S latitude in a. the North Pacific, b. the South Pacific, c. the North Atlantic, and d. the South Atlantic estimated in GlobColour-GSM (black), GlobColour-AVM (red), ESA-OC-CCI-v5.0 (blue). Straight lines are deseasonalized linear trends, respectively.

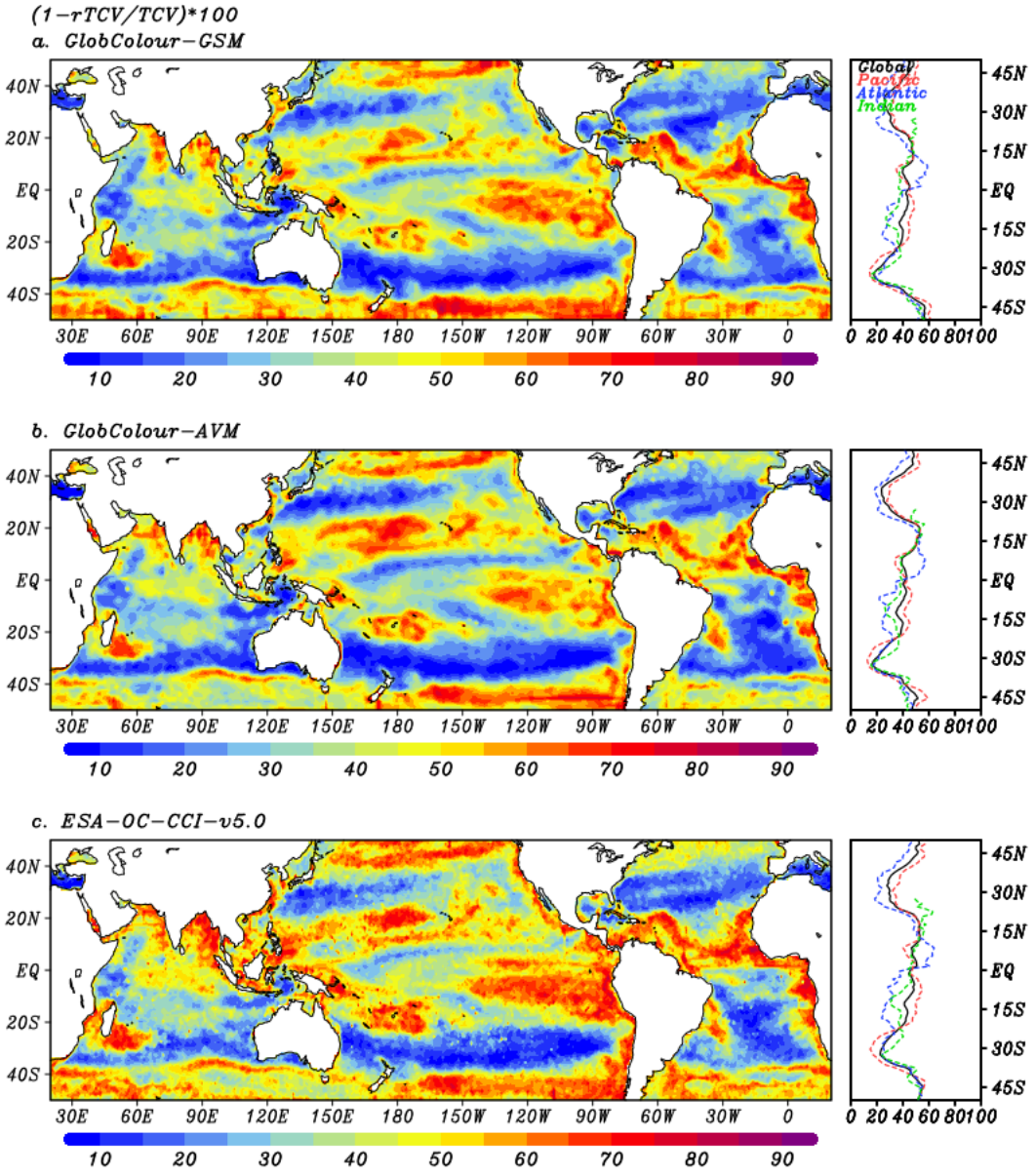

Figure S7. Residuals of explained TCV by rTCV in a. GlobColour-GSM, b. GlobColour-AVM, and c. ESA-OC-CCI-v5.0.

Supporting table

Table S1. Indication of lead-time for statistical predictability of Fig. 5: lagged seasonal timeseries input ($\boldsymbol{\tau}$) of climate indices to calculate rCHLa_predic.

Leadtime	Training input of lagged timeseries (averaged lag month) of climate indicies into MLR model for calculating rCHLa_predic			
	$\boldsymbol{\tau}$ =1	$\boldsymbol{\tau}$ =2	$\boldsymbol{\tau}$ =3	$\boldsymbol{\tau}$ =4
1 month	1-3 lag month	4-6 lag month	7-9 lag month	10-12 lag month
2 month	2-3 lag month	4-6 lag month	7-9 lag month	10-12 lag month
3 month	3 lag month	4-6 lag month	7-9 lag month	10-12 lag month
4 month		4-6 lag month	7-9 lag month	10-12 lag month
5 month		5-6 lag month	7-9 lag month	10-12 lag month
6 month		6 lag month	7-9 lag month	10-12 lag month
7 month			7-9 lag month	10-12 lag month
8 month			8-9 lag month	10-12 lag month
9 month			9 lag month	10-12 lag month
10 month				10-12 lag month
11 month				11-12 lag month
12 month				12 lag month